Analyst

Accepted Manuscript

ROYAL SOCIETY OF CHEMISTRY

www.rsc.org/analyst

Sensitive and selective determination of hydroxychloroquine in the presence of uric acid using a new nanostructure self-assembled monolayer modified electrode: Optimization by multivariate data analysis

Asma Khoobi, Sayed Mehdi Ghoreishi*, Mohsen Behpour

Department of Analytical Chemistry, Faculty of Chemistry, University of Kashan, Kashan P.O. Box 87317-51167 I.R. Iran

Abstract

A highly sensitive electrochemical nanosensor was developed using covalent modification of glassy carbon electrode (GCE) by self-assembly of a novel Schiff base. Scanning electron microscopy (SEM) and electrochemical techniques were used to investigate the immobilization of the self-assembled monolayer (SAM) on the GCE. The electrochemical behavior of hydroxychloroquine (HCQ) in the presence of uric acid (UA) at the surface of modified electrode was studied using differential pulse voltammetry (DPV) technique. Response surface methodology (RSM) is used to optimize various operating variables involved pH, immersion time, scan rate, step potential and modulation amplitude on the voltammetric response of HCQ. RSM is formulating a mathematical model which correlates the independent parameters with the peak current of HCQ. The central composite rotatable design (CCRD) has been applied to conduct the experiments. Then, under the optimized conditions, HCQ was determined in the presence of UA. The electrochemical measurements demonstrated that this biosensor responded

* *Sayed Mehdi Ghoreishi, Ph. D.*
Department of Analytical Chemistry, Faculty of Chemistry, University of Kashan, Kashan, I.R. Iran.
Phone number: +983615912395
Fax number: +983615552930
E-mail address: s.m.ghoreishi@kashanu.ac.ir

well to HCQ, confirming that the self-assembly immobilization method was effective. Also, the interference, the storage stability, and the reproducibility of the biosensor were studied and assessed. The developed nanosensor was economical and efficient, making it potentially attractive for the application to real sample analysis.

Keywords: Nanosensor, Self-assembled monolayer, Hydroxychloroquine, Uric acid, Electrochemistry, Experimental design, Response surface methodology

1. Introduction

Hydroxychloroquine, 2-[N-4-{(7-chloroquinolin-4-yl)amino}pentyl-N-ethyl]amino ethanol, (HCQ) has been shown to inhibit a variety of viral infections and decrease immune reactivity.[1] These effects are mediated by a change in intracellular pH which inhibits viral and cellular enzymes involved in activation. HCQ can be applied in the treatment of acute attacks and suppressive of Malaria vivax, Plasmodium ovale, and suitable strains of Plasmodium falciparum, Plasmodium malaria, systemic and discoid Lupus erythematosus and rheumatoid arthritis.[2] It also, suppresses human immunodeficiency virus type-1 (HIV-1) replicating into vitro in T-cells and monocytes by inhibiting post-transcriptional modifications of the virus.[3] So far, few electrochemical techniques have been applied for the study of chloroquine drugs.[4-6] Arguelho et al.[4] presented electrochemical reduction of HCQ using glassy carbon electrode (GCE). They reported a linear concentration range from 2×10^{-5} to 5×10^{-4} M, with a detection limit of 11.2 μg mL^{-1} for HCQ. Mashhadizadeh et al.[5] investigated an electroanalytical methodology for the determination of chloroquine using DPV at a $Cu(OH)_2$ nano-wire-

modified carbon paste electrode. Based on the paper chloroquine showed a linear range from 0.068 to 6.88 μg mL^{-1} with a detection limit of 0.01μg mL^{-1}. Recently, Deroco et al. [6] reported a square wave voltammetry (SWV) method for the determination of HCQ with a cathodically pretreated boron-doped diamond electrode. In the research, obtained SWV analytical curve presented a linear response from 0.1 to 1.9 μmol L^{-1}, with a detection limit of 0.06 μmol L^{-1}.

Uric acid (2,6,8-trihydroxypurine, UA) is the end product of endogenous and dietary purine nucleotide metabolism in humans. It is derived from xanthine, which, in turn, results from hypoxanthine, being both reactions catalyzed by xanthine oxidase. In most species, UA is further metabolized to allantoin by the urate oxidase enzyme, but humans lack this enzyme because of a defective gene that is not transcribed. Therefore, UA is excreted in urine, and plasma UA levels in humans are significantly higher as compared to those in most mammals.[7] Because HCQ and UA usually can be coexist together in living systems, there is an interest in the development of methods for their determination; and also, these compounds are easily oxidized, the development of electrochemical-based biosensors is considered absolutely important. The main drawbacks associated with conventional electrode materials for electrochemical sensing of these compounds are poor selectivity due to overlapping oxidation peaks and low reproducibility arising from electrode fouling.[8] Furthermore, biosensing needs the controlled immobilization of biomolecules in close contact with electrochemical transducers. Self-assembled monolayers (SAMs) give a unique tunable platform since the thickness of the organic films and surface properties are adjustable to suit different sensing applications.[9]

Generally, use of SAMs permits the biochemical reaction to carry on in a more controlled manner thus enhancing biosensing parameters.[10]

Optimization by the traditional 'one-factor-at-a-time' method requires a considerable amount of experimental run and time. An alternate strategy is a statistical approach, e.g. design of experiment (DOE) and response surface methodology (RSM).[11-13] The RSM achieves multiple regression analysis to determine the relationship between the process variables and response. It needs less number of experiments in order to generate essential information for a statistically acceptable result.[14] Additionally, the RSM finds its application in the optimization of industrial processes.[15]

Herein, we report the fabrication of a nanosensor based on the self-assembly of a novel Schiff base film which has been bound to the surface of GCE for the first time. The results revealed that the SAM modified electrode shows higher electrocatalytic activity compared with the bare GCE. The oxidation peak of UA was completely diminished while the differential pulse peak current of HCQ was not altered by the presence of a high concentration of UA at the SAM modified electrode. Scanning electron microscopy (SEM), cyclic voltammetry (CV) and electrochemical impedance spectroscopy (EIS) techniques were used for the characterization of the modified electrode. Analytical performance of the modified biosensor was demonstrated by selective detection of HCQ in the presence and UA. Also, other novelty of the present paper was simultaneous optimization of all effective variables on HCQ voltammetric response using RSM, employing a five-level, five-variable CCRD. Based on this, a new electrochemical method was developed for the determination of HCQ, demonstrating with human blood serum samples.

2. Materials and methods

2.1. Reagents and chemicals

All preparations of the aqueous solutions, polishing of the electrodes and cleaning of the glassware were performed using deionized (DI) water. Chemicals used were $K_3Fe(CN)_6$, $K_4Fe(CN)_6$, HCQ, UA, phosphoric acid (H_3PO_4), acetic acid (CH_3COOH), boric acid (H_3BO_3), sodium hydroxide (NaOH) and all other reagents were purchased from MERCK (Germany). All chemicals were reagent grade and were used as received without further purification. All electrochemical experiments were carried out at room temperature (25±1ºC).

2.2. Instrumentation

EIS measurements were performed using an Autolab Potentiostat/Galvanostat PGSTAT30 (Eco Chemie, Utrecht, The Netherlands) which is controlled the General Purpose Electrochemical System (GPES 4.9,006 software) and the NOVA 1.8 software (Metrohm Autolab). Impedance spectra were recorded in a background solution of 5.0 mM of the $K_3Fe(CN)_6$ + $K_4Fe(CN)_6$ in phosphate buffer (PB) (pH 7.0) at a formal potential. The alternating voltage was 10.0 mV and the frequency range was 1.0×10^{-1} to 1.0×10^{4} Hz. A modified Randles' model, in which double layer capacitance (C_{dl}) was replaced by a constant phase element (CPE), was applied to expound the impedances achieved in the whole frequency range, from which analytical information were extracted.[16] Voltammetric measurements were carried out by SAMA 500 (electroanalyzer system, Islamic Republic of Iran). A personal computer (Pentium IV) was used for data

storage and processing. A conventional three-electrode electrochemical cell was applied for all electrochemical experiments with a bare or the modified GCE (1 mm in diameter, Metrohm, Switzerland) as the working electrode, an Ag/AgCl (3.0 M KCl) as the reference electrode and a platinum electrode as the counter electrode. All the potential given in this paper were referred to the reference electrode. SEM images were performed using a KYKY-EM3200. A magnetic stirrer was applied when necessary. A digital pH meter (Metrohm model 691) was used when preparing buffer solutions that served as the supporting electrolyte in the electrochemical experiments. DI water was prepared by an ultra pure water system type smart-2-pure, TKA, Germany. An ultrasonic bath (Sonorex Digital, 10P, Bandelin) was used for cleaning the GCE.

2.3. Synthesis of Schiff base

N-[(E)-1-(2-pyridyl)methylidene]-N(3-{[(E)-1-(2-pyridyl)methylidene]amino} propyl) amine (PAPA) as a new Schiff base, was prepared according to the literature through a well known procedure,[17] as follows: pyridine-2-carbaldehyde (2.14 g, 0.02 mol) was mixed with 50.0 mL distilled methanol in 250.0 mL round bottom flask, which was stirred using a magnetic stirrer. Propane-1,3-diamine solution (0.01 mol), dissolved in 30.0 mL of distilled methanol was added drop by drop using a dropping funnel to the above solution. The contents were refluxed for 5 h, and then cooled at room temperature. The reddish brown solid product was filtered, and the product was re-crystallized from methanol. Analytical calculated for PAPA C, 71.40; H, 6.39; N, 22.21. Found: C, 71.03; H, 6.38; N, 22.33%.^{1}H-NMR (400 MHz) chemical shift 8.79 (s, 2H, -CH=N-), 7.10-8.63

(m, 8H, aromatic), 3.65 (m, 4H, CH_2), 4.53 (m, 2H, CH_2) ppm. Selective IR bands (cm^{-1}), KBr pellets, (C=N), 1587; (C=C), 1662 cm^{-1}.

2.4. Preparation of the biosensor

The bare GCE was polished successively with 0.3 and 0.05 μm aqueous slurries of alumina before modification, rinsed with DI water, and sonicated in ethanol and DI water for 5 min, respectively. Then, it cleaned electrochemically by cycling the electrode potential between -0.1 and +1.3 V vs. the reference electrode, with a 100 mV s^{-1} scan rate in 0.1 M sulfuric acid until reproducible voltammograms were observed. The cleaned GCE was immersed in 1.0 mM PAPA ethanol solution for 13 h (at room temperature), was washed thoroughly with DI water to remove unadsorbed materials from the electrode surface and then a GC/PAPA SAM-modified electrode was used as a biosensor for detection of HCQ in the presence of UA.

2.5. Experimental design and statistical analysis

In the present work, for determination of HCQ in the presence of UA, RSM was used. RSM is a collection of mathematical and statistical methods that are suitable for modeling and analysis of problems when a response is controlled by several variables. Before applying the RSM methodology, it is first necessary to choose an experimental design. However, CCRD is a useful design for optimization of the effective parameters and analyzes the interaction between the variables with a minimum number of experiments. This design consists of three parts: (1) a full factorial or fractional factorial design; (2) an additional design, often a star design in which experimental points are at a

distance α from its center; and (3) a central point (Fig. 1). Full uniformly rotatable central composite designs present the following characteristics: (1) they require an experiment number according to $N = 2^f + 2f + r$, where *f* is the number of factors and *r* is the replicate number of the central point; (2) α-values depend on the number of variables and can be calculated $\alpha = \pm 2^{f/4}$; (3) all factors are studied in five levels.[18] Therefore, a 5-factor (f = 5), 5-level (Table 1) test comprising 45 experiments was designed for investigation of DPV response of HCQ. The response behavior could be related to the selected independent factors by a second-order polynomial. The generalized response surface model is shown by Eq. (1):

$$Y = \beta_0 + \sum_{i=1}^{5} \beta_i X_i + \sum_{i=1}^{5} \beta_{ii} X_i^2 + \sum_{i=1}^{5} \sum_{j=i+1}^{5} \beta_{ij} X_i X_j + \varepsilon \quad (1)$$

where, Y is the predicted response, β_o is the coefficient for intercept (constant), β_i is the coefficient of linear effect, β_{ii} is the coefficient of quadratic effect, β_{ij} is the coefficient of interaction effect, ε is a term that describes other sources of variability not accounted for the response function; x_i and x_j are coded predictor independent variables. The coefficients of the regression model were estimated by fitting the experimental results using MINITAB Release 16, developed by Minitab Inc. (USA), a statistical software package. The significance level 95% was set for the mathematical model and surface response.

3. Results and discussion

3.1. PAPA immobilization on GCE

3.1.1. Surface morphology of the SAM film

The homogeneity of SAM is critical for the purpose of electroanalytical applications. The surface morphology of the GC/PAPA SAM modified electrode was characterized by SEM in order to compare the bare and modified electrodes. The SEM images of the bare GC and GC/PAPA SAM modified electrodes are shown in Fig. 2A[19] and B, respectively. As shown in Fig. 2B, PAPA film was equably modified onto the GCE. These results indicate that PAPA could be fixed to the GCE to form the PAPA self-assembly GCE.

3.1.2. Electrochemical characterization of the SAM film

The cyclic voltammeric measurements were performed in a 5.0 mM the redox probe ($K_3Fe(CN)_6$ + $K_4Fe(CN)_6$) PB solution at a scanning rate of 100.0 mV s^{-1}. In order to investigation of pH effect on the structure of the monolayer on GCE, cyclic voltammograms of the bare and modified GCE were recorded in different pHs. Fig .3A shows the cyclic voltammograms for the bare GCE in pH 3.0, 6.0 and 8.0. As can be observed, the bare GCE gives good reversibility with a pair of well-defined voltammetric peaks. Fig. 3B illustrates the cyclic voltammograms for the GC/PAPA SAM modified electrode after immersion in 1.0 mM PAPA ethanol solution for 13 h in the same pHs. The curves become much more irreversible at the surface of modified electrode. It is probable that the immobilized PAPA forms an almost insulating layer on the electrode and electrons cannot be freely transferred to the electrode. Also, the effect of pH on the cyclic voltammograms can be explained by the following reason: when positively or negatively charged SAMs are formed, electrostatic interactions between charged surface and charged probe affect the aforementioned parameters, and the resultant of the interactions will establish apparent response of the surface.[20] At the surface of GC/PAPA

SAM modified electrode an increase in the faradic currents can be due the electrostatic attraction between positively charged PAPA monolayer and negatively charged probe in test solution at pH 3.0 (Fig. 3B, curve a). But, the assembled PAPA layer is deprotonated at pH 8.0 and the GCE surface is negatively charged. Therefore, the faradic currents for the probe redox reaction were decreased and an irreversible behavior is expected due to the electrostatic repulsion between the surface of GC/PAPA SAM electrode and the negatively charged probe in the solution (Fig. 3B, curve c).

In order to get more information about the surface, EIS technique was also used. It is well known that EIS is an effective tool for studying the interface properties of surface modified electrodes. The typical electrochemical interface can be represented as an electrical circuit[21] as shown in Fig. 4A. R_{ct}, which equals the semicircle diameter at higher frequencies in the Nyquist plot, controls the interfacial electron transfer rate of the redox probe between the solution and the electrode. Thus, R_{ct} can be applied to describe the interface properties of the electrode. This value varies when different substances are adsorbed onto the electrode surface. The complex plane plots obtained on GC/PAPA SAM electrode in the presence of 5.0 mM $K_3Fe(CN)_6$ + $K_4Fe(CN)_6$ in acidic and alkaline solutions, pH 3.0, 6.0 and 8.0 are exhibited in Fig. 4B. The diameter of the Nyquist circles increase at the surface of GC/PAPA SAM modified electrode (the plots for the bare GC have not shown). These results are in agreement with the cyclic voltammeric measurements. Thus, the interfacial electron transfer is retarded, resulting in an increase in the electron transfer resistance. In order to investigation of pH effect, the R_{ct} values were estimated using CPE equivalent circuit model. These values for GC and GC/PAPA SAM electrodes are 36.0 and 111.7 Ω at pH 3.0, 45.5 and 550.4 Ω at pH 6.0 and 53.5 and

1836.8 Ω, at pH 8.0, respectively. By comparisons of results, it seems that at pH 3.0 (Fig. 4B, curve a); the R_{ct} was increased by a factor of 3.1 from bare GCE to GC/PAPA SAM electrode and more irreversible behavior is observed. The apparent change in R_{ct} is the resultant of (a) insulating effect of the SAM film, (b) opening behavior of SAM and (c) high electrostatic attraction between the positively charged SAM surface and negatively charged probe, with dominant effect of electrostatic attraction.[16] These results were in good agreement with CV studies. At pH 8.0 (Fig. 4B, curve c); the R_{ct} was increased by a factor of 30 from bare GCE to GC/PAPA SAM electrode. This difference is from the increase of electrostatic repulsion between negatively charged electrode surface and negatively charged probe, and partially from the thickness of SAM film. These behaviors are also in good agreement with those obtained by CV at pH 8.0.

3.1.3. Immersion time effect on the SAM formation

Adsorption behavior of PAPA at the surface of GCE as a function of time was investigated by the EIS technique. Fig. 5 shows the complex plane plots achieved on GCE after different immersion times in 1.0 mM ethanolic PAPA. As can be observed, the R_{ct} values fluctuate by time. At primary immersion times the R_{ct} values are low (before 4.0 h immersion), and then this value is increased (by 6.0 h immersion), after secondly decreases the stable state is achieved (after 8.0 h immersion). On the other hand, the R_{ct} pass through a transient state and reach to a relatively more stable state. The first fast kinetic step is easily observable before 2.0 h immersion of the clean GCE in Schiff base solution. Afterwards, several disordered/adsorption occurs, until the SAM gets its final

state. Therefore, it is seemed that after 8.0 h of immersion time, the SAM will be stable and suitable as a biosensor.

3.2. Application of the modified electrode as a biosensor

3.2.1. Optimization studies using CCRD and RSM

One of the main purposes of the work is sensitive determination of HCQ in the presence of UA. For achieving the purpose, all effective variables on the DPV response of HCQ containing pH (X_1), immersion time (X_2), scan rate (X_3), step potential (X_4) and modulation amplitude (X_5) were optimized simultaneously using RSM based on CCRD. Therefore, the DPV experiments were performed according to the CCRD matrix given in Table 2. Then the optimum coded value of each variable was obtained from MINITAB® Release 16 software. These coded values and corresponding actual (uncoded) values are shown in Table 3. Also, by the graphical representations of the regression Eq. (8) that called the response surfaces and the contour plots, optimized value of each factor is obtained (Fig. 6 (A,B)).

3.2.2. CV characterization of the HCQ biosensor

In the present study, GCE was modified with PAPA SAM. Fig. 7 shows the cyclic voltammograms of 0.5 μM HCQ on the bare GC and GC/PAPA SAM modified electrodes in pH 7.6 Britton-Robinson (B-R) buffer solution with a scan rate of 0.1 V s^{-1}. As can be seen, HCQ shows two oxidation peaks. But, the first anodic peak did not show enough sensitivity and therefore, the second anodic peak was applied in the further studies. It can be clearly seen that, HCQ shows a relatively broad and weak oxidation

peak at 988.0 mV (curve b). However, when PAPA was immobilized on the GCE surface, the oxidation peak becomes well-defined, with amagnification 2.4 times greater than the bare GCE and a negative potential shift of 46.0 mV. The lower overpotential and the increase in current response are clear evidence of the catalytic effect of the modified electrode on the oxidation of HCQ.

3.2.3. Electrochemical response of the biosensor to HCQ

Under the optimum conditions, the oxidation peak currents of various HCQ concentrations at the GC/PAPA SAM modified electrode were recorded by DPV technique. Fig. 8A illustrates the effect of various HCQ concentrations on the differential pulse voltammograms at the modified electrode. Using the GC/PAPA SAM electrode well-defined voltammograms were obtained and the height of the anodic peak increased with increasing of the concentrations. Fig. 8B is the calibration curve for determination of HCQ. The oxidation peak current of HCQ was proportional to its concentration in the range of 5.0×10^{-8}-12.3×10^{-6} M. Calibration equation can be described as follows: I_p (μA) = 0.2079 C (μM) + 0.1130, with a correlation coefficient of 0.9961. According to the rules of IUPAC,[22] based on a signal-to-noise ratio of 3 (S/N=3), the detection limit was calculated to be 4.5 nM for HCQ.

3.2.4. Determination of HCQ in the presence of UA

The selective determination of HCQ in the presence of UA has been investigated using DPV technique. For achieving this purpose, voltammograms of a mixture of HCQ and UA on the bare and GC/PAPA SAM modified electrodes were recorded. Fig. 9 shows the

differential pulse voltammograms obtained for a mixture containing 28.0 μM HCQ and 100.0 μM UA at the bare and GC/PAPA SAM modified electrodes in 0.2 M B-R buffer solution (pH 7.6). As can be observed, at the bare GCE (Fig. 9, curve b), the oxidation peaks of HCQ and UA appear at 954.0 mV and 248.0 mV, respectively. Whereas in these conditions the oxidation peak currents of HCQ and UA were achieved at 1.13 μA and 0.49 μA, respectively. But, at the GC/PAPA SAM modified electrode (Fig. 9, curve c), the oxidation peaks of HCQ and UA appeared at 906.0 mV and 194.0 mV, respectively. Furthermore, HCQ showed an about 2.4-fold increased anodic current response, whereas UA represented an about 1.7-fold decreased anodic current response. These results indicate that modification of the GCE causes both increasing of sensitivity for HCQ and decreasing interference of UA for HCQ redox. Therefore, it is seemed at the surface of GC/PAPA SAM modified electrode, sensitive and selective determination of HCQ in the presence of UA is possible. According to these results, differential pulse voltammograms of a mixture containing different amounts of HCQ in the presence of 100.0 μM UA were recorded (Fig. 10A). The calibration plot of HCQ in the presence of UA at the GC/PAPA SAM modified electrode under optimal experimental conditions was illustrated in the Fig. 10B. As expected, the response of the biosensor to HCQ was linear in the range from 7.4×10^{-8} M to 11.9×10^{-6} M (I_p (μA) = 0.1990 C (μM) + 0.1301, R^2 = 0.9964) with a detection limit of 4.7 nM (S/N=3). Therefore, even high concentration of UA has not strongly interfere in the determination of low concentration of HCQ.

3.2.5. Figures of merit and application of the method

In order to estimate the performance and feasibility of the methodology, the novel modified electrode was tested by applying it to the measurement of HCQ concentration in real samples. In this case under the optimum conditions, the proposed GC/PAPA SAM modified electrode was used to the measurement of HCQ concentration in human blood serum. During DPV experiments, definite volume of serum was injected into 0.2 M, B-R buffer solution (pH 7.6) containing GC/PAPA SAM modified electrode. The standard addition method was adopted to demonstrate the possibility of HCQ detection in real samples. The obtained results were presented in Table 4. Based on Table 4 the GC/PAPA SAM modified electrode exhibits an excellent average recovery of 101.91% for HCQ determination in human serum. The determination of HCQ in human serum with excellent recovery shows validates the pertinent nature of PAPA film for the sensor applications.

3.2.6. Interference research

The response of the proposed sensor to some common interference was investigated by addition of various interferences to 0.2 M, B-R buffer solution (pH 7.6) in the presence of 0.5 μM HCQ. From these analysis it is found that no interference occurred in the presence of substance as following: 500-fold K^+, NH_4^+, Na^+, Zn^{2+}, Cl^-, CO_3^{2-}, SO_4^{2-} and glycine, 100-fold L-alanine, 50-fold L-phenylalanine and 3,4-dihydroxy phenyl alanine, with the deviations below 5% (Fig. 1S). These results show that the GC/PAPA SAM modified electrode has selectivity to HCQ and its selectivity cannot be easily perturbed.

3.2.7. The repeatability and stability of the SAM film

In order to demonstrate the precision and practicability of the proposed method, the repeatability and storage stability of the GC/PAPA SAM modified electrode were investigated by DPV technique. The relative standard deviation of the modified electrode response to 5.0 μM HCQ was 2.57% after twenty successive measurements, showing excellent repeatability of the modified biosensor. As a further demonstration of the stability, the modified electrode was also investigated by measuring the current response of 5.0 μM HCQ, once every day. The current retained 94.3% of its original response after 5 days. The phenomenon indicated the good stability of the GC/PAPA SAM modified electrode.

4. Conclusions

A new nanosensor was developed for the determination of HCQ in the presence of UA based on PAPA self-assembled monolayer electrode. The GC/PAPA SAM modified electrode was characterized by SEM, CV and EIS techniques. A design of experiments methodology was followed to evaluate the importance of the various parameters involved on voltammetric response of HCQ. Using DPV a linear relationship as 7.4×10^{-8} - 11.9×10^{-6} M with a detection limit of 4.7×10^{-9} M was observed for the determination of HCQ in the presence of UA in the optimized conditions. The developed nanosensor was applied successfully for the determination of HCQ in human blood serum. The advantages of easy preparation of sensor, simple instrumentation and low detection limit will make the system useful in fabrication of simple devices for determination of HCQ in the presence of UA.

Acknowledgments

The authors are grateful to University of Kashan for supporting this work by Grant No. 211037-8.

References

1 V. Roberto, A. Tiziano and A. Serozh, *European Patent EP1374867*, 2004.

2 A. Gringauz, Introduction to Medicinal Chemistry-How Drugs Act and Why, Wiley-VCH, Inc., New York, NY, 1997.

3 K. Sperber, M. Louiea, T. Krausa, J. Proner, E. Sapira, S. Lin, V. Stecher and L. Mayer, *Clin. Ther.*, 1995, **17**, 622.

4 M.L.P.M. Arguelho, J.F. Andrade and N.R. Stradiotto, *J. Pharm. Biomed. Anal.*, 2003, **32**, 269.

5 M.H. Mashhadizadeh and M. Akbarian, *Talanta*, **2009**, 78, 1440.

6 P.B. Deroco, F.C. Vicentini, G.G. Oliveira, R.C. Rocha-Filho and O. Fatibello-Filho, *J. Electroanal. Chem.*, **2014**, 71, 19.

7 K.M. Kim, G.N. Henderson, X. Ouyang , R.F. Frye , Y.Y. Sautin , D.I. Feig and R.J. Johnson, *J. Chromatogr. B*, 2009, **877**, 2032.

8 Z.Q. Gao and H. Huang, *Chem. Commun.*, 1998, **19**, 2107.

9 Z. Dai and H. Ju, Phys. *Chem. Chem. Phys.*, 2001, **3**, 3769.

10 F. Frederix, K. Bonroy, W. Laureyn, G. Reekmans, A. Campitelli, W. Dehaen and G. Maes, *Langmuir*, 2003, **19**, 4351.

11 A. Khoobi, S.M. Ghoreishi, S. Masoum and M. Behpour, *Bioelectrochemistry*, 2013, **94**, 100.

12 R.E. Bruns, I.S. Scarminio and B.B. Neto, Statistical Design Chemometrics, Elsevier, Amsterdam; 2006.

13 S.M. Ghoreishi, M. Behpour, A. Khoobi and Z. Moghadam, *Anal. Lett.*, 2013, **46**, 323.

14 J. Fermoso, M.V. Gil, B. Arias, M.G. Plaza, C. Pevida, J.J. Pis and F. Rubiera,. *Int. J. Hydrogen Energy*, 2010, **35**, 11912.

15 R.O. Kuehl, Design of experiments: statistical principles of research design and analysis. 2nd ed. California: Brooks/Cole; 2000.

16 R.K. Shervedani and S.A. Mozaffari, *Anal. Chim. Acta*, 2006, **562**, 223.

17 R. Hahn, W.A. Herrmann, G.R.J. Artus and M. Kleine, *Polyhedron*, 1995, **14**, 2953.

18 R.G. Brereton, Applied Chemometrics for Scientists, John Wiley & Sons, Ltd, 2007.

19 Y. Oztekin, Z. Yazicigil, A. Ramanaviciene and Ramanavicius, *Sens. Actuators, B*, 2011;**152**, 37.

20 Y.Y. Jun and K.S. Beng, *Electrochem. Commun.*, 2004, **6**, 87.

21 J. Randles, *Faraday Discuss.*, 1947, **1**, 11.

22 J. Inczédy, T. Lengyel and A.M. Ure, IUPAC, Compendium of Analytical Nomenclature: Definitive Rules 1997, 3rd ed., Blackwell Science, Oxford; 1998.

Table captions

Table 1. Independent factors and their levels used in the response surface design.

Table 2. Experimental design and the results for DPV response of HCQ at the surface of GC/PAPA SAM modified electrode.

Table 3. Optimum values of the variables obtained from RSM.

Table 4. The testing results of spiked human blood serum on the GC/PAPA SAM modified biosensor (n = 3).

Figure captions

Fig. 1. Representation of a three factor, two level design in CCRD.

Graphical representation of the CCRD.

Fig. 2. SEM images of the (a) bare GCE and (b) PAPA film formed on the GCE.

Fig. 3. Cyclic voltammograms of 5. 0 mM $K_3Fe(CN)_6$ + $K_4Fe(CN)_6$ in (a) pH 3.0, (b) pH 6.0 and (c) pH 8.0 and PB solution (A) at the bare GCE and (B) at the GC/PAPA SAM modified electrode. Scanning rate: 100.0 mV s^{-1}.

Fig. 4. (A) Equivalent electric network of the electrochemical interface: R_s, C_{dl}, R_{ct} and Z_w are electrolyte resistance, double-layer capacitance, charge transfer resistance and Warburg impedance, respectively. (B) Nyquist diagram of EIS containing 5.0 mM $K_3Fe(CN)_6$ + $K_4Fe(CN)_6$ in PB solution at the GC/PAPA SAM modified electrode in (a) pH 3.0, (b) pH 6.0 and (c) pH 8.0. AC potential 10.0 mV, DC potential +0.2 V, frequency range 0.1-10000 Hz.

Fig. 5. Complex plane plots obtained on GC/PAPA SAM modified electrode in the presence of 5.0 mM $K_3Fe(CN)_6$ + $K_4Fe(CN)_6$ after different immersion times in the Schiff base solution. Conditions: AC potential 10.0 mV, DC potential +0.2 V, frequency range 0.1-10000 Hz.

Fig. 6. Response surface plot (A) and its corresponding contour plot (B) of HCQ response as function of pH (X_1), immersion time (X_2), scan rate (X_3), step potential (X_4) and modulation amplitude (X_5).

Fig. 7. Cyclic voltammograms of 0.2 M B-R buffer solution at, (a) GC/PAPA SAM modified electrode, (b) and (c) in the presence of 0.5 μM HCQ at GC and GC/PAPA SAM modified electrodes, respectively.

Fig. 8. (A) Differential pulse voltammograms of the GC/PAPA SAM modified electrode in 0.2 M B-R buffer solution containing different concentrations of HCQ (a-i corresponding to: 0.05, 0.12, 0.50, 0.99, 1.96, 2.44, 3.85, 6.54 and 12.28 μM) in the optimized conditions. (B) The calibration curve for the determination of HCQ.

Fig. 9. Differential pulse voltammograms of 0.2 M B-R buffer solution (a) at GC/PAPA SAM modified electrode, (b) and (c) containing 28.0 μM HCQ + 100.0 μM UA, on the bare and GC/PAPA SAM modified electrodes, respectively in the optimized conditions.

Fig. 10. (A): DPV of GC/PAPA SAM modified electrode in 0.2 M B-R buffer solution containing 100.0 μM UA and different concentrations of HCQ containing a-i corresponding to: 0.07, 0.12, 0.52, 0.91, 1.67, 2.31, 4.76, 6.54 and 11.89 μM, (B): I (μA) as a function of HCQ concentration (μM).

Table 1

Operating variables	Levels				
	-2.38	***-1***	***0***	***+1***	***+2.38***
X_1: pH	6.0	7.0	8.0	9.0	10.0
X_2: Immersion time (h)	4.0	8.0	12.0	16.0	20.0
X_3: Scan rate (V s^{-1})	0.02	0.06	0.10	0.14	0.18
X_4: Step potential (V)	0.001	0.002	0.003	0.004	0.005
X_5: Modulation amplitude (V)	0.01	0.03	0.05	0.07	0.9

Table 2

Run	Design matrix					Response (I / μA)
	X_1	X_2	X_3	X_4	X_5	Y
1	-1	1	1	-1	-1	0.1940
2	-1	1	-1	1	1	0.0246
3	0	0	0	2.378	0	0.1509
4	0	0	0	-2.378	0	0.3131
5	-1	-1	1	1	-1	0.0706
6	-1	-1	1	-1	-1	0.1950
7	-1	1	1	1	1	0.0155
8	1	-1	1	1	1	0.0412
9	1	1	-1	-1	-1	0.1801
10	1	-1	-1	-1	-1	0.1560
11	-1	-1	-1	1	-1	0.1647
12	-1	-1	-1	-1	1	0.0979
13	0	0	0	0	0	0.2868
14	1	1	-1	1	-1	0.0893
15	-2.378	0	0	0	0	0.1113
16	1	1	1	-1	-1	0.2151
17	2.378	0	0	0	0	0.0493
18	0	0	0	0	-2.378	0.1734
19	0	0	-2.378	0	0	0.1134
20	1	-1	-1	1	1	0.0165
21	-1	1	1	1	-1	0.1745
22	-1	1	-1	-1	1	0.1985
23	0	-2.378	0	0	0	0.0524
24	1	1	-1	-1	1	0.0925
25	-1	1	-1	-1	-1	0.2211
26	1	1	-1	1	1	0.0133
27	0	2.378	0	0	0	0.0125
28	-1	-1	-1	1	1	0.0099
29	0	0	2.378	0	0	0.0385
30	0	0	0	0	0	0.2284
31	1	1	1	1	1	0.0319
32	-1	-1	1	1	1	0.0180
33	1	-1	1	-1	1	0.1065
34	-1	-1	-1	-1	-1	0.2163
35	1	-1	1	-1	-1	0.1163
36	-1	1	1	-1	1	0.1099
37	-1	-1	1	-1	1	0.0379
38	1	1	1	1	-1	0.1183
39	1	-1	-1	-1	1	0.1485
40	-1	1	-1	1	-1	0.0858
41	1	-1	-1	1	-1	0.1732
42	0	0	0	0	0	0.2735
43	0	0	0	0	2.378	0.0137
44	1	1	1	-1	1	0.0994
45	1	-1	1	1	-1	0.1061

Table 3

Variables	Coded optimized values	Actual optimized values
pH	-0.408	7.6
Immersion time (h)	0.264	12.91
Scan rate (V s^{-1})	-0.360	0.087
Step potential (V)	-2.378	0.001
Modulation amplitude (V)	-0.456	0.042

Table 4

Sample	Added (μM)	found (μM)	Recovery (%)
1	0.00	Not detected	_
2	0.30	0.32	106.67
3	0.70	0.68	97.14

Fig. 1

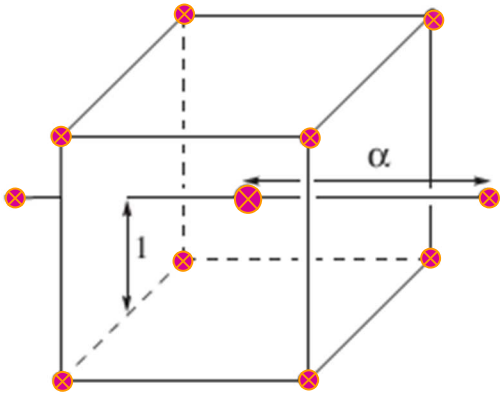

Fig. 2

(A)

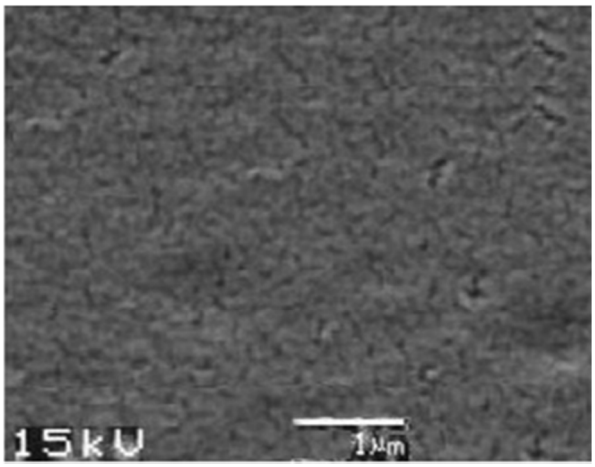

(B)

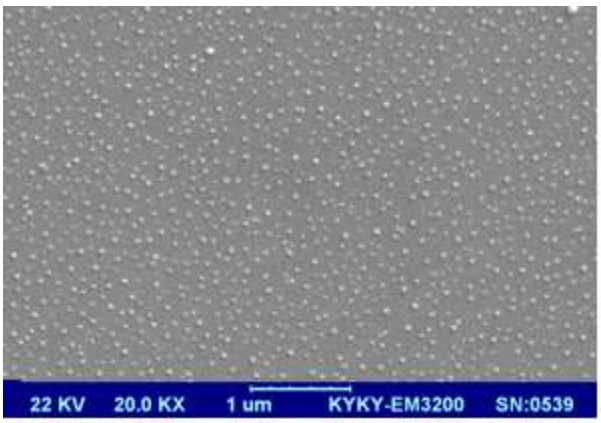

Fig. 3

(A)

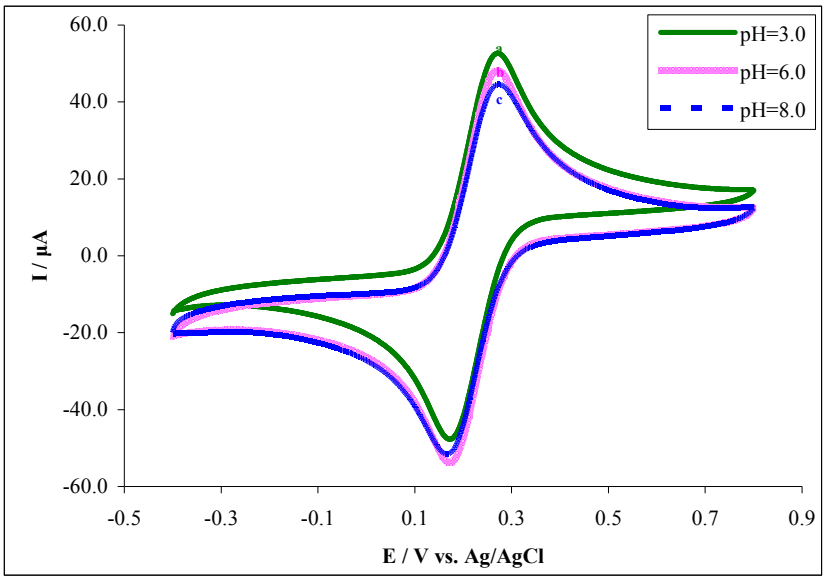

(B)

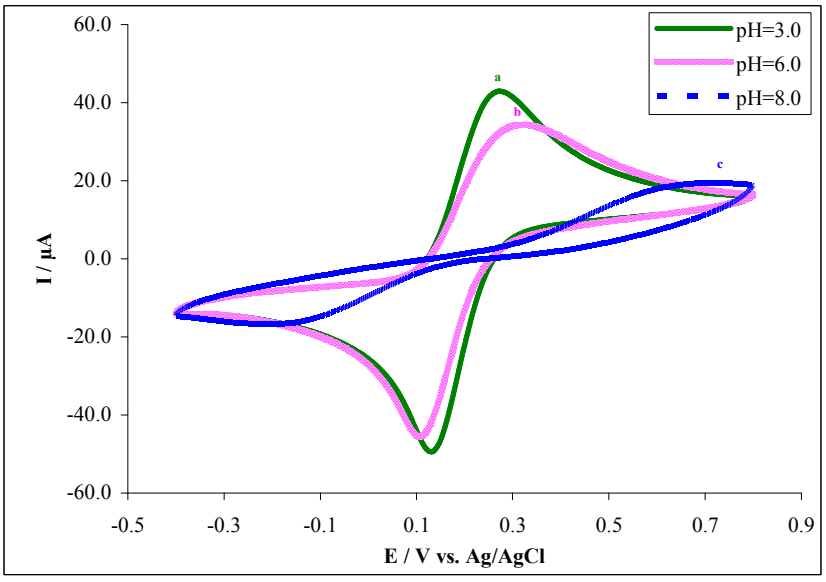

Fig. 4

(A)

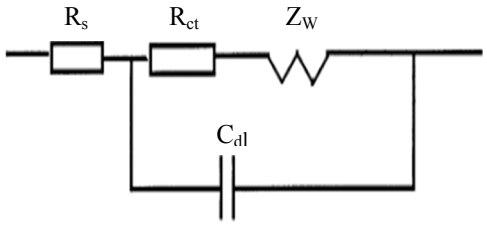

(B)

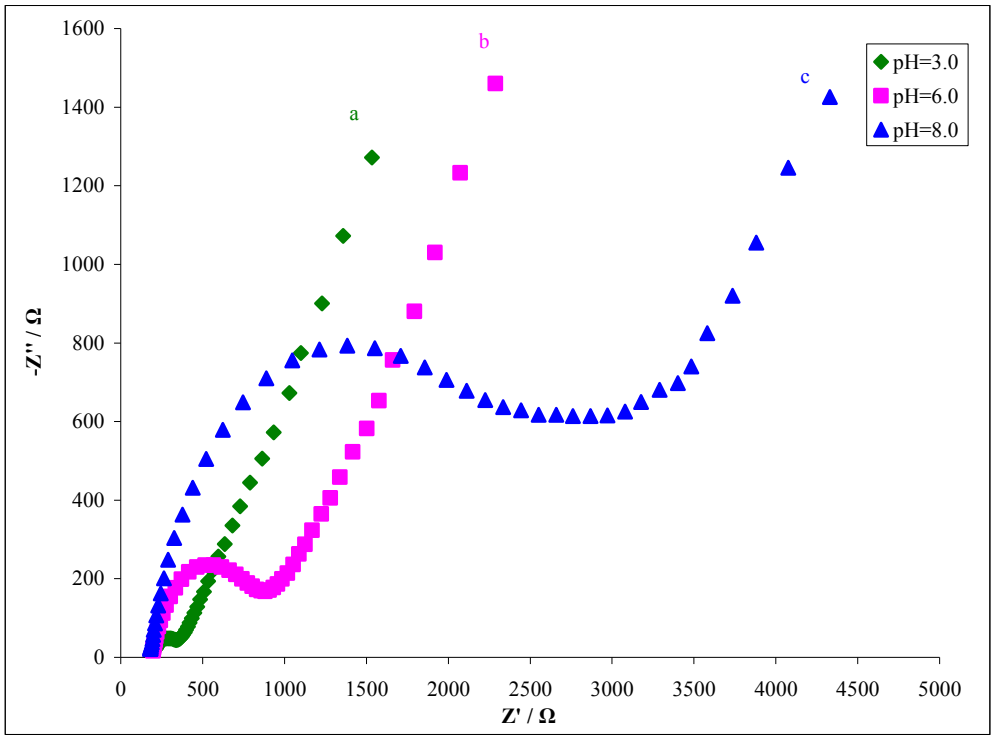

Fig. 5

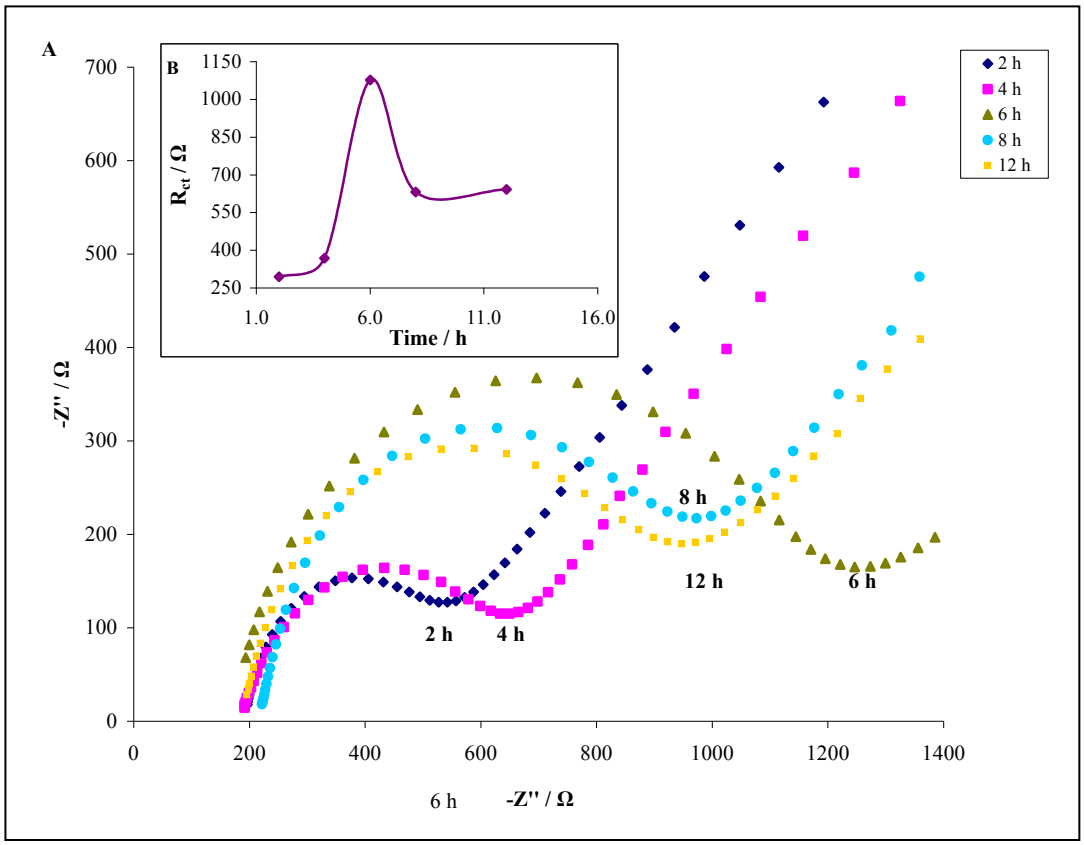

Fig. 6

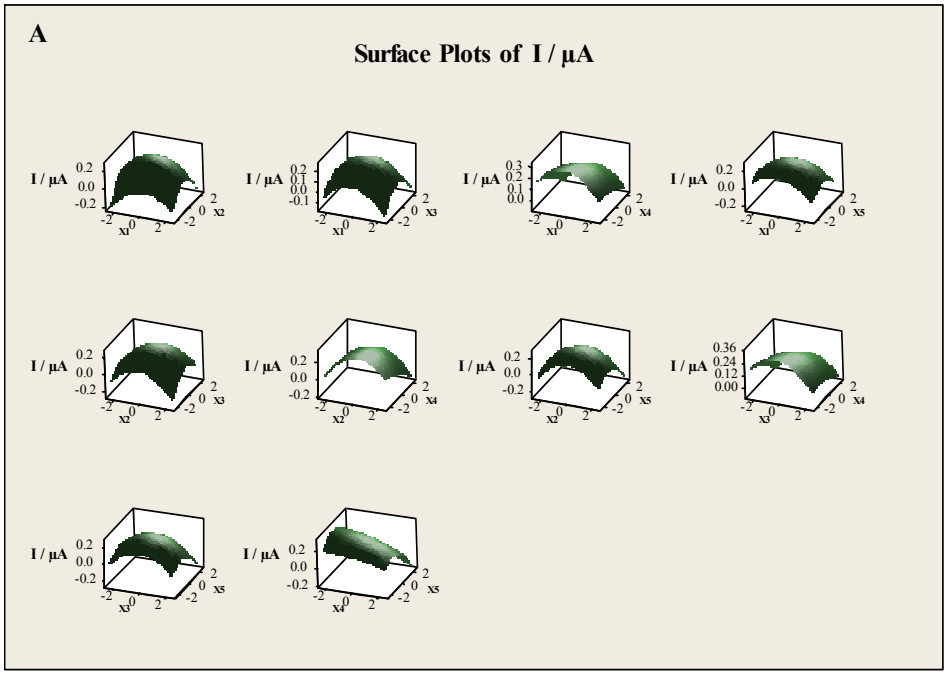

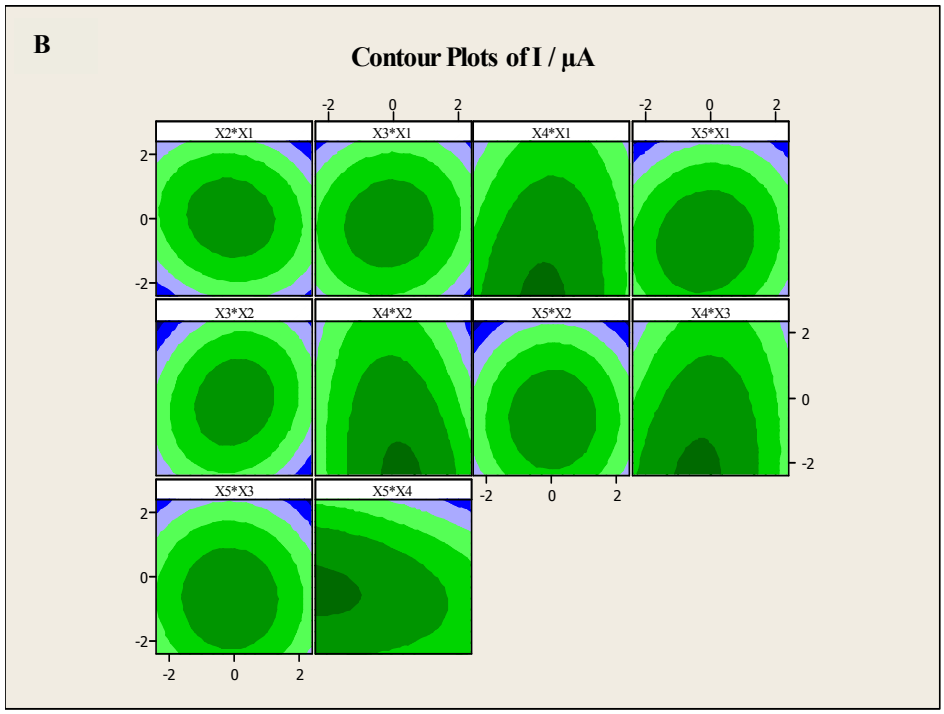

Fig. 7

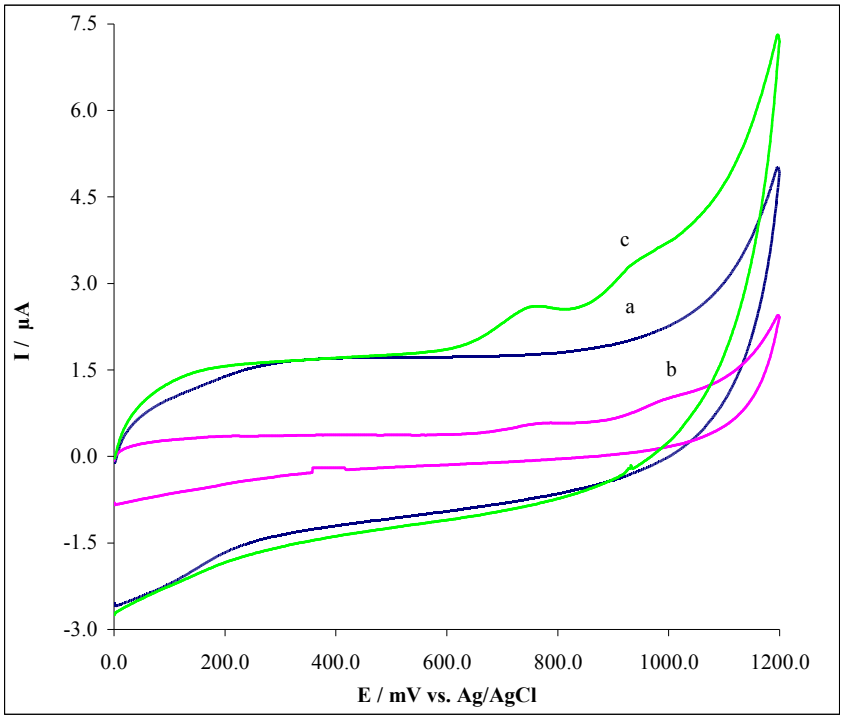

Fig. 8

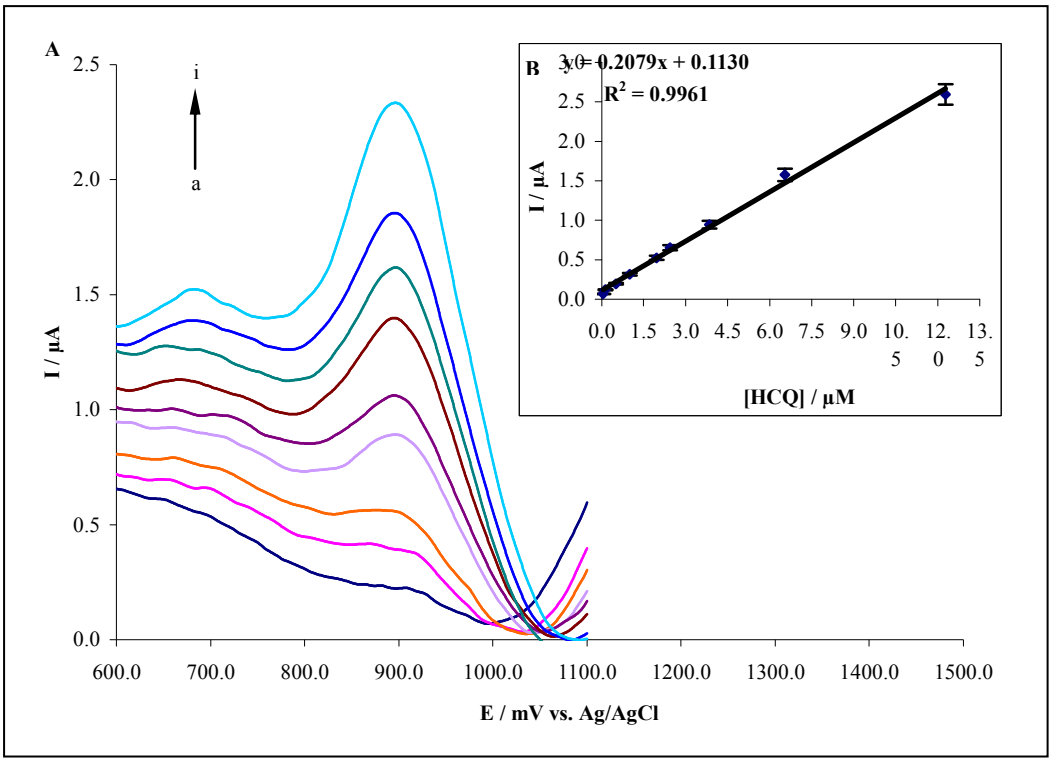

Fig. 9

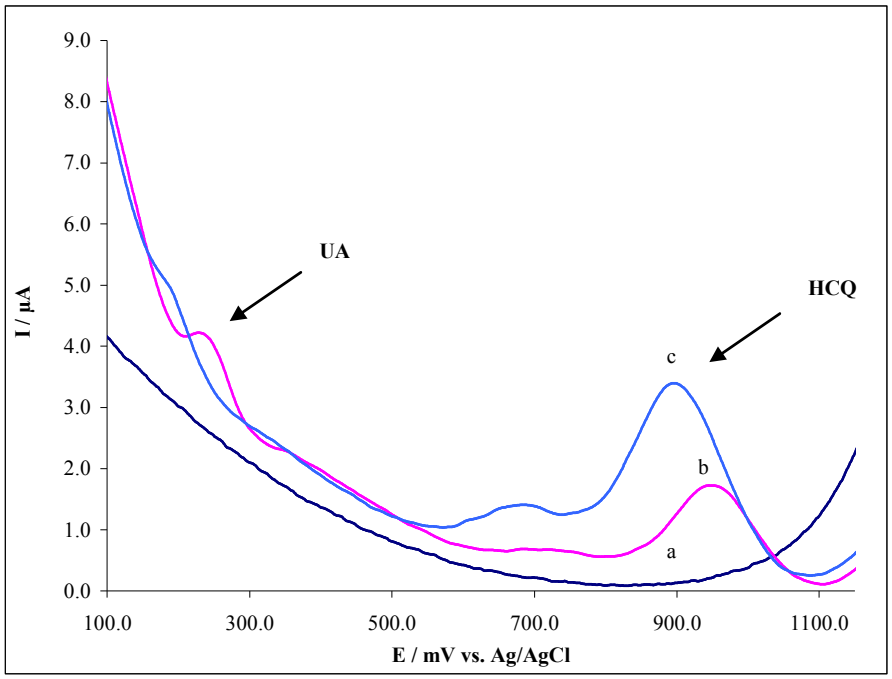

Fig. 10